

LETTER TO THE EDITOR

Post common envelope binaries from SDSS

VIII. Evidence for disrupted magnetic braking[★]

M. R. Schreiber¹, B. T. Gänsicke², A. Rebassa-Mansergas^{1,2}, A. Nebot Gomez-Moran³, J. Southworth^{2,4},
A. D. Schwope³, M. Müller³, C. Papadaki⁵, S. Pyrzas^{2,6}, A. Rabitz³, P. Rodríguez-Gil^{6,7,8}, L. Schmidtobreick⁹,
R. Schwarz³, C. Tappert¹, O. Toloza¹, J. Vogel³, and M. Zorotovic^{9,10}

¹ Departamento de Física y Astronomía, Facultad de Ciencias, Universidad de Valparaíso, Valparaíso, Chile
e-mail: matthias@dfa.uv.cl

² Department of Physics, University of Warwick, Coventry, CV4 7AL, UK

³ Astrophysikalisches Institut Potsdam, An der Sternwarte 16, 14482 Potsdam, Germany

⁴ Department of Physics and Chemistry, Keele University, Staffordshire, ST5 5BG, UK

⁵ Institute of Astronomy & Astrophysics, National Observatory of Athens, 15236 Athens, Greece

⁶ Isaac Newton Group of Telescopes, Apartado de correos 321, S/C de la Palma, 38700, Canary Islands, Spain

⁷ Instituto de Astrofísica de Canarias, Vía Láctea, s/n, 38205 La Laguna, Spain

⁸ Departamento de Astrofísica, Universidad de La Laguna, 38206 La Laguna, Tenerife, Spain

⁹ European Southern Observatory, Alonso de Cordova 3107, Santiago, Chile

¹⁰ Departamento de Física y Astronomía, Facultad de Ciencias, Pont. Universidad Católica, Santiago, Chile

Received 4 January 2010 / Accepted 15 March 2010

ABSTRACT

Context. The standard prescription of angular momentum loss in compact binaries assumes magnetic braking to be very efficient as long as the secondary star has a radiative core, but to be negligible if the secondary star is fully convective. This prescription has been developed to explain the orbital period gap observed in the orbital period distribution of cataclysmic variables but has so far not been independently tested. Because the evolutionary time-scale of post common envelope binaries (PCEBs) crucially depends on the rate of angular momentum loss, a fundamental prediction of the disrupted magnetic braking theory is that the relative number of PCEBs should dramatically decrease for companion-star masses exceeding the mass that corresponds to the fully-convective boundary.

Aims. We present the results of a large survey of PCEBs among white dwarf/main sequence (WDMS) binaries that allows us to determine the fraction of PCEBs as a function of secondary star mass and therewith to ultimately test the disrupted magnetic braking hypothesis.

Methods. We obtained multiple spectroscopic observations spread over at least two nights for 670 WDMS binaries. Systems showing at least 3σ radial velocity variations are considered to be strong PCEB candidates. Taking into account observational selection effects we compare our results with the predictions of binary population simulations.

Results. Among the 670 WDMS binaries we find 205 strong PCEB candidates. The fraction of PCEBs among WDMS binaries peaks around $M_{\text{sec}} \sim 0.25 M_{\odot}$ and steeply drops towards higher mass secondary stars in the range of $M_{\text{sec}} = 0.25\text{--}0.4 M_{\odot}$.

Conclusions. The decrease of the number of PCEBs at the fully convective boundary strongly suggests that the evolutionary time scales of PCEBs containing fully convective secondaries are significantly longer than those of PCEBs with secondaries containing a radiative core. This is consistent with significantly reduced magnetic wind braking of fully convective stars as predicted by the disrupted magnetic braking scenario.

Key words. binaries: close – magnetic fields – stars: low mass – white dwarfs

1. Introduction

The formation and evolution of virtually all close compact binaries, including cataclysmic variables (CVs) and low mass X-ray binaries is driven by orbital angular momentum loss due to gravitational radiation and – probably much stronger – magnetic braking. While gravitational radiation has been proven to be correctly described by Einstein's quadrupole formula (Taylor et al. 1979), current prescriptions of magnetic braking differ by up to four orders of magnitude.

The standard theory of angular momentum loss due to magnetic braking in close compact binaries, known as disrupted magnetic braking (DMB), was developed in the early eighties. Based on Skumanich's (1972) analysis of the spin down rates of G-type stars, Verbunt & Zwaan (1981) derived a prescription for angular momentum loss due to magnetic braking of the form $\dot{J} \propto P_{\text{orb}}^{-3}$. In order to explain the orbital period gap observed in the period distribution of CVs, i.e. a statistically significant deficit of systems with $2 \text{ h} \lesssim P_{\text{orb}} \lesssim 3 \text{ h}$, Rappaport et al. (1983) proposed the DMB scenario by assuming that magnetic braking ceases when the secondary star becomes fully convective at $M_{\text{sec}} \sim 0.2\text{--}0.3 M_{\odot}$ – which, for a Roche-lobe filling secondary star corresponds to $P_{\text{orb}} \sim 3 \text{ h}$. In the DMB scenario the donor

[★] RV tables are only available in electronic form at the CDS via anonymous ftp to cdsarc.u-strasbg.fr (130.79.128.5) or via <http://cdsweb.u-strasbg.fr/cgi-bin/qcat?J/A+A/513/L7>

stars in CVs above the gap are driven out of thermal equilibrium by strong mass transfer caused by efficient magnetic braking.

At the upper edge of the gap, the secondary star in a CV becomes fully convective. Disrupted magnetic braking causes the mass loss rate to drop and the donor star to relax to its thermal equilibrium radius, which is smaller than its Roche-lobe radius. The CV turns into a non-interacting detached white dwarf plus main sequence (WDMS) binary, and its evolution towards shorter P_{orb} is now only driven by angular momentum loss through gravitational radiation. At $P_{\text{orb}} \approx 2$ h, the Roche lobe shrinks sufficiently far to restart mass transfer. Designed to explain the period gap, additional support for the DMB scenario comes from (1) the secular mean accretion rates derived from accretion induced compressional heating that are systematically higher above than below the gap (Townsend & Bildsten 2003; Townsend & Gänsicke 2009), and (2) the donor stars in CVs above the gap that appear slightly expanded with respect to their main-sequence radii, which is consistent with the donor stars being out of thermal equilibrium (Knigge 2006).

Nevertheless, the DMB hypothesis remains an ad-hoc assumption. Although there is now some evidence for a discontinuity in the braking of single stars around the fully convective boundary (Bouvier 2007; Reiners & Basri 2008), it is not entirely clear if the DMB scenario correctly describes magnetic braking in single stars. In addition, the DMB idea is not backed-up by a thorough theory describing the interactions between rotation, magnetic field generation, and wind braking for low mass stars. Recent results indicate that the field topology changes at the fully convective boundary (Reiners & Basri 2009; Saunders et al. 2009), but whether this may indeed cause magnetic braking to become inefficient remains an open question. In this letter we present new and strong observational evidence for DMB.

2. Testing magnetic braking with PCEBs

Schreiber & Gänsicke (2003) realised that observational population studies of the progenitors of CVs, i.e. detached post common envelope binaries (PCEBs) consisting of a white dwarf primary and an M-dwarf companion, could lead to new constraints on magnetic braking. Politano & Weiler (2006) recently proposed a definite and concrete test of DMB: if magnetic braking is indeed disrupted at the fully convective boundary ($M_{\text{sec}} \sim 0.3 M_{\odot}$), the evolutionary time-scales prior to the onset of accretion should be much longer for PCEBs with fully convective secondaries compared to those with secondaries above that boundary. Consequently, one should expect to find more PCEBs with fully convective secondary stars. More specifically, Politano & Weiler (2006) predict that the relative number of PCEBs should abruptly decrease by ~ 37 – 73% at the fully convective boundary. If in contrast magnetic braking is at work in secondary stars as proposed by e.g. Andronov et al. (2003), the relative number of PCEBs should depend little on the mass of the secondary star, with no abrupt change at the fully convective boundary.

Carrying out this test of the DMB model, i.e. measuring the relative number of PCEBs among WDMS binaries as a function of the secondary mass, requires a large sample of PCEBs, which is only now becoming available because of the efficiency of the Sloan Digital Sky Survey spectroscopy (SDSS, Adelman-McCarthy et al. 2008; Abazajian et al. 2009; Yanny et al. 2009) in discovering WDMS binaries (e.g. Smolčić et al. 2004; Silvestri et al. 2007; Rebassa-Mansergas et al. 2007; Schreiber et al. 2007; Rebassa-Mansergas et al. 2010). The population of SDSS WDMS binaries contains wide systems whose

stellar components did not interact and thus evolved like single stars, and close binaries that suffered from dynamically unstable mass transfer, i.e. PCEBs. We are carrying out a dedicated follow-up observing program with the aim to identify the PCEBs among the SDSS WDMS binaries, and to determine their binary parameters. First results on individual systems have been published by Schreiber et al. (2008); Rebassa-Mansergas et al. (2008); Pyrzas et al. (2009); Nebot Gómez-Morán et al. (2009); Schwöpe et al. (2009). Here we present radial velocity studies of 670 SDSS WDMS binaries, identify 205 strong PCEB candidates and determine the fraction of PCEBs among WDMS binaries, henceforth $N_{\text{PCEB}}/N_{\text{WDMS}}$, as a function of secondary mass.

3. Observations

We carried out extensive follow-up observations of the most complete published sample of WDMS binaries (based on SDSS Data Release 6, Rebassa-Mansergas et al. 2010), obtaining at least two spectra per system, spread over at least two nights. At the time of writing (January 2010) we obtained a total of 3308 spectra for 670 SDSS WDMS binaries. The design of the observations and data reduction as well as the radial velocity measurements of the secondary stars, primarily based on the $\text{Na I } \lambda\lambda 8183.27, 8194.81$ absorption doublet, are described in detail in Gänsicke et al. (2010, MNRAS, in prep.) and Nebot Gomez-Moran et al. (2010, A&A, in prep.)

The observational results are summarized in Table 1 which is electronically available at the Centre de Données astronomiques de Strasbourg (CDS). We tested the 670 systems for radial velocity variations using a χ^2 test, i.e. the measured radial velocities were tested against the hypothesis of a constant radial velocity. Systems showing radial velocity variations with a confidence level of at least 0.9973 (henceforth 3σ) are identified as strong PCEB candidates, systems with less significant variations are considered as wide WDMS candidates, i.e. systems where the two stars did not undergo any interaction during their evolution. Stellar parameters of the 670 systems (masses and spectral types for the white dwarf and secondary star and the distance to the binary) were taken from Rebassa-Mansergas et al. (2010) and Nebot Gomez-Moran (2010, A&A, in prep.) and are provided in Table 2 available at the CDS. The peak-to-peak radial velocity variations of the PCEB candidates range from ~ 25 – 450 km s^{-1} , corresponding to maximum binary separations of $a \sim 1$ – $150 R_{\odot}$ and maximum orbital periods of ~ 2 h– 160 days. In a parallel effort we measured the orbital periods of a representative subsample consisting of 60 PCEBs that have been identified through our $\geq 3\sigma$ radial velocity criterion and find that all these systems have orbital periods shorter than four days, the vast majority ($\sim 90\%$) even shorter than one day (Gänsicke et al. 2010, MNRAS, in prep.). We therefore here assume that all the PCEB candidates are synchronised and circularised short period close binary systems.

4. PCEB fraction among SDSS WDMS binaries

Our large set of strong PCEB candidates and WDMS binaries that are most likely wide systems provides the potential to test the DMB hypothesis. The distributions of the PCEB candidates and the entire WDMS binary sample are shown as a function of secondary spectral type in the bottom left panel of Fig. 1. Performing a χ^2 test of the PCEB candidate against the wide candidate distribution we find that the null-hypothesis can be rejected with 99.997% confidence. Thus the secondary spectral

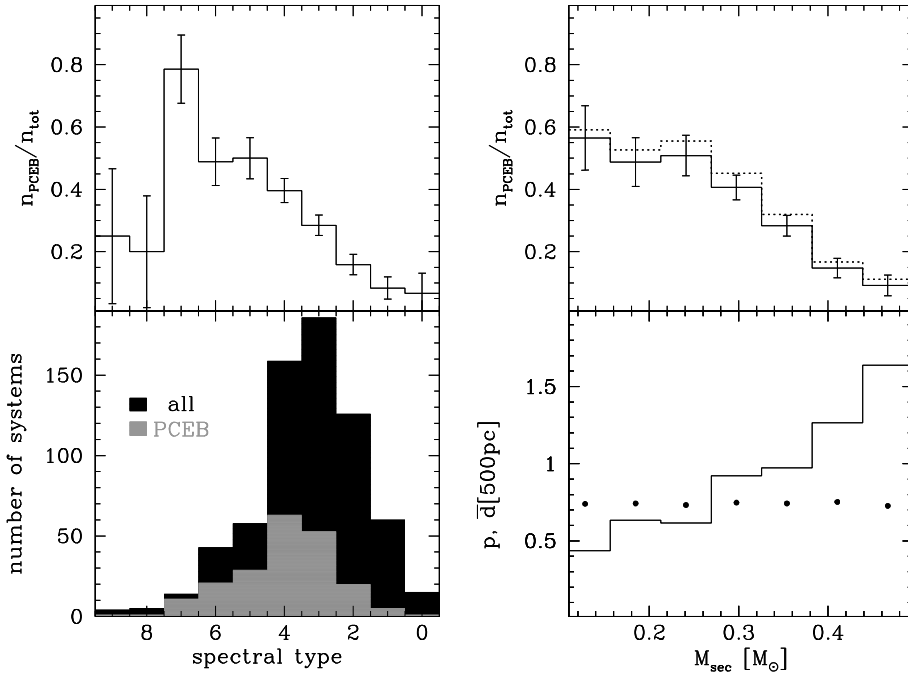


Fig. 1. Distributions of WDMS binaries that have at least two radial velocity measurements separated by at least one day. The left bottom panel shows the distributions of systems with at least 3σ radial velocity variations (gray) and all the 670 systems (black) as a function of secondary star spectral type. According to a χ^2 test, the distributions of wide candidates and PCEB candidates are different with a confidence level of 99.997%. The top left panel provides the distribution of PCEBs among SDSS WDMS binaries ($N_{\text{PCEB}}/N_{\text{WDMS}}$). Selection effects are shown in the bottom right panel. Black dots represent the average PCEB detection probabilities p for each mass bin. The histogram provides the average distance \bar{d} for each mass bin. Our final result, $N_{\text{PCEB}}/N_{\text{WDMS}}$ as a function of secondary mass is given in the top right panel. The bias corrected (dotted line) and the measured fractions (solid line) are very similar. We find an obvious and steep decrease of the number of PCEBs in the range of secondary masses of $M_{\text{sec}} = 0.25\text{--}0.4 M_{\odot}$. Note that the right hand side panels contain less bins because the masses of M0–M1 respectively M7–M9 secondary stars are very similar.

type distributions of wide WDMS binary candidates and PCEB candidates are intrinsically different. $N_{\text{PCEB}}/N_{\text{WDMS}}$ as a function of secondary spectral type is shown in the top left panel of Fig. 1. Apparently, the fraction of PCEBs is very low ($<20\%$) for M0–M2 secondary stars, significantly increases around spectral types M3–M4, and finally exceeds $\sim 50\%$ for M5–M7 secondary stars. At M7 $\sim 75\%$ of the observed systems are strong PCEB candidates. For the latest M dwarf secondaries (M8–M9) our data are subject to low number statistics, but it seems that the PCEB fraction again drops below $\sim 50\%$.

In a second step we used the spectral type-mass relation of Rebassa-Mansergas et al. (2007) to derive $N_{\text{PCEB}}/N_{\text{WDMS}}$ as a function of secondary mass (solid line in the top right panel of Fig. 1). Because the masses of M0–M1 respectively M7–M9 secondary stars are very similar, this distribution contains just seven bins. The measured fraction of PCEBs is steeply decreasing towards higher mass secondaries in the range of $M_{\text{sec}} = 0.25\text{--}0.4 M_{\odot}$, but stays at about 50% for lower mass secondaries.

5. Selection effects

A first general note is that the SDSS sample of WDMS binaries is not complete and probably subject to selection effects in various stellar parameters like white dwarf temperature or secondary mass. Given that these effects will affect PCEBs and wide WDMS binaries in the same way our choice of investigating $N_{\text{PCEB}}/N_{\text{WDMS}}$ as a function of M_{sec} is independent of these selection effects. However, there are two possible observational biases which may skew $N_{\text{PCEB}}/N_{\text{WDMS}}$, i.e. selection effects within the target algorithm of the SDSS spectroscopy that is used to identify WDMS binaries in the first place, and selection effects that might be introduced through the design of our follow-up programme that affect PCEBs and wide WDMS binaries in a different way. These will be discussed below.

The algorithm selecting objects for SDSS fibre spectroscopy may introduce a subtle bias affecting $N_{\text{PCEB}}/N_{\text{WDMS}}$ as a function of apparent magnitude and hence of secondary mass that needs to be evaluated. The majority of the WDMS binaries are serendipitously picked up by fibres allocated to objects that have

non-stellar colours, i.e. colours that differ from single main sequence stars and white dwarfs. Because of their composite spectral energy distributions, WDMS binaries appear as objects with non-stellar colours within SDSS as long as they are not spatially resolved by the typical seeing of $\approx 1''$. Those WDMS binaries that are spatially resolved will have star-like colours for each component, and are unlikely to obtain an SDSS fibre spectrum. The $15 \lesssim g \lesssim 20$ magnitude limit of SDSS spectroscopy and of our follow-up programme implies that the average distance to SDSS WDMS binaries increases with absolute magnitude – and hence with the mass of the secondary star. Figure 1 (bottom right) illustrates this effect, the average distance of the WDMS binaries in the sample discussed here increases from ~ 220 pc for $M_{\text{sec}} \sim 0.1 M_{\odot}$ to ~ 820 pc for $M_{\text{sec}} \sim 0.45 M_{\odot}$. Hence, intrinsically faint WDMS binaries have on average a higher chance to be spatially resolved than bright ones, and would consequently not be targeted for SDSS follow-up spectroscopy, introducing a *bias towards low-mass secondaries* in $N_{\text{PCEB}}/N_{\text{WDMS}}$. Assuming an average spatial resolution of $1''$ and the average distances from above (Fig. 1, bottom right) translate into minimum projected separations of resolved WDMS binaries ranging from ≥ 220 AU for the lowest mass bin to ≥ 820 AU for the highest mass bin. Assuming binary separations of $3 R_{\odot} \leq a \leq 10^6 R_{\odot}$ (e.g. Willems & Kolb 2004), and taking into account that the initial distribution of binary separations a is supposed to decrease with increasing a , i.e. $dN/da \propto a^{-1}$ (Popova et al. 1982), we estimate that the fraction of wide WDMS binaries that are spatially resolved by SDSS is decreasing from $\sim 23\%$ at $M_{\text{sec}} \sim 0.1 M_{\odot}$ to $\sim 12\%$ at $M_{\text{sec}} \sim 0.45 M_{\odot}$.

The finite spectral resolution and the details of the temporal sampling of our follow-up radial velocity studies will prevent us from identifying some genuine PCEBs within the observed sample of WDMS binaries. To evaluate this selection effect, we calculated the average PCEB detection probability p for each secondary mass bin. Taking into account the times of observations and the stellar masses, we performed Monte-Carlo simulations similar to those presented in Gänsicke et al. (2010, MNRAS in prep.), i.e. for typical PCEB orbital periods (2 h–2 days) we randomly selected 10 000 times the phases and an inclination

for each system and calculated the corresponding radial velocities. Averaging over the orbital period the fraction of $>3\sigma$ radial velocity variations gives the average PCEB detection probability for each system. The PCEB detection probabilities averaged over all systems that fall in a certain mass bin are given as black dots in the bottom right panel of Fig. 1. Because the average detection probabilities are nearly constant as a function of M_{sec} , $p \sim 0.7$, the number of genuine PCEBs missed by our follow-up programme are simply proportional to the number of PCEBs that we did identify, leading to a *bias against PCEBs with low mass companions* in $N_{\text{PCEB}}/N_{\text{WDMS}}$. We used the calculated PCEB detection probabilities to find the most likely fraction of PCEBs for each mass bin using Bayes' theorem according to Maxted et al. (2000) and indeed found an even steeper decline in the range of secondary masses corresponding to the fully convective boundary.

Interestingly, the two selection effects related to the spatial resolution of SDSS and to our spectral resolution and temporal sampling nearly cancel each other out: the dotted histogram in the top right panel of Fig. 1 shows the bias-corrected fraction of PCEBs among WDMS binaries, which is very similar to the measured one (solid line histogram in the same panel). We therefore conclude that the intrinsic fraction of PCEBs among WDMS binaries does indeed decrease significantly in the range of $M_{\text{sec}} = 0.25\text{--}0.4 M_{\odot}$.

6. Discussion

Overall, our result agrees well with the main prediction of Politano & Weiler (2006) for DMB. We find the fraction of PCEBs steeply decreasing by $\sim 80\%$ in the secondary mass range that corresponds to the fully convective boundary, and only the DMB prescription predicts this decrease. While this is an important finding, it is worth to keep in mind that Politano & Weiler (2006) calculated the relative number of PCEBs as a function of M_{sec} , which is not identical to $N_{\text{PCEB}}/N_{\text{WDMS}}$ measured here. To derive the predicted $N_{\text{PCEB}}/N_{\text{WDMS}}$, one needs to divide the relative number of PCEBs by the assumed secondary mass function. As the pairing algorithm used by Politano & Weiler (2006) predicts the number of WDMS binaries to smoothly increase with secondary mass (Kouwenhoven et al. 2009), the decrease of $N_{\text{PCEB}}/N_{\text{WDMS}}$ predicted by their simulations is $>37\text{--}73\%$ in agreement with the $\sim 80\%$ measured here.

Comparing the predictions of Politano & Weiler (2006) and our observational result in more detail, we find that the measured decrease in $N_{\text{PCEB}}/N_{\text{WDMS}}$ is slightly broader than the predicted one. This can easily be understood as resulting from uncertainties in the spectral type determination and the spectral type mass relation. Both uncertainties contribute to the uncertainty of the secondary mass determination, which naturally causes any steep gradient to be smeared out.

7. Conclusion

We have measured the fraction of PCEBs among white dwarf/main sequence binaries identified by the SDSS and found a steep decrease at the secondary star mass corresponding to the fully convective boundary, i.e. there are substantially less PCEBs with secondaries that have a radiative core. This result agrees excellently with the disrupted magnetic braking scenario that

predicts significantly longer evolutionary timescales for PCEBs containing fully convective secondary stars. We therefore conclude that magnetic braking is disrupted, or is at least significantly reduced at the fully convective boundary. According to recent magnetic field measurements of M-dwarfs, this might be caused by changes of the magnetic field topology at the fully convective boundary.

Acknowledgements. We acknowledge support from FONDECYT (grant 1061199, MRS), ESO/Comite Mixto, Gemini/Conicyt (grant 32080023, ARM) and DLR (FKZ 50OR0404, ANGM). This paper includes data collected at (1) ESO Paranal and La Silla, Chile under programme IDs 083.D-0862, 082.D-0507, 080.D-0407, 079.D-0531, 078.D-0719, (2) the Gemini Observatory, which is operated by the Association of Universities for Research in Astronomy, Inc., under a cooperative agreement with the NSF on behalf of the Gemini partnership: the NSF (United States), the STFC (United Kingdom), the NRC (Canada), CONICYT (Chile), the ARC (Australia), MCT (Brazil) and MINCYT (Argentina), (3) Las Campanas Observatory, Chile with the 6.5 m Magellan Telescopes, (4) the Spanish Observatorio del Roque de los Muchachos of the Instituto de Astrofísica de Canarias with the WHT, which is operated on the island of La Palma by the Isaac Newton Group, and (5) at the Centro Astronómico Hispano Alemán (CAHA) at Calar Alto, operated jointly by the Max-Planck Institut für Astronomie and the Instituto de Astrofísica de Andalucía (CSIC).

References

- Abazajian, K. N., Adelman-McCarthy, J. K., Agüeros, M. A., et al. 2009, *ApJS*, 182, 543
- Adelman-McCarthy, J. K., Agüeros, M. A., Allam, S. S., et al. 2008, *ApJS*, 175, 297
- Andronov, N., Pinsonneault, M., & Sills, A. 2003, *ApJ*, 582, 358
- Bouvier, J. 2007, in *IAU Symposium*, ed. J. Bouvier, & I. Appenzeller, IAU Symp., 243, 231
- Knigge, C. 2006, *MNRAS*, 373, 484
- Kouwenhoven, M. B. N., Brown, A. G. A., Goodwin, S. P., Portegies Zwart, S. F., & Kaper, L. 2009, *A&A*, 493, 979
- Maxted, P. F. L., Marsh, T. R., & Moran, C. K. J. 2000, *MNRAS*, 319, 305
- Nebot Gómez-Morán, A., Schwöpe, A. D., Schreiber, M. R., et al. 2009, *A&A*, 495, 561
- Politano, M., & Weiler, K. P. 2006, *ApJ*, 641, L137
- Popova, E. I., Tutukov, A. V., & Yungelson, L. R. 1982, *Ap&SS*, 88, 55
- Pyrzas, S., Gänsicke, B. T., Marsh, T. R., et al. 2009, *MNRAS*, 394, 978
- Rappaport, S., Joss, P. C., & Verbunt, F. 1983, *ApJ*, 275, 713
- Rebassa-Mansergas, A., Gänsicke, B. T., Rodríguez-Gil, P., Schreiber, M. R., & Koester, D. 2007, *MNRAS*, 382, 1377
- Rebassa-Mansergas, A., Gänsicke, B. T., Schreiber, M. R., et al. 2008, *MNRAS*, 390, 1635
- Rebassa-Mansergas, A., Gänsicke, B. T., Schreiber, M. R., Koester, D., & Rodríguez-Gil, P. 2010, *MNRAS*, 406, 620
- Reiners, A., & Basri, G. 2008, *ApJ*, 684, 1390
- Reiners, A., & Basri, G. 2009, *A&A*, 496, 787
- Saunders, E. S., Naylor, T., Mayne, N., & Littlefair, S. P. 2009, *MNRAS*, 397, 405
- Schreiber, M. R., & Gänsicke, B. T. 2003, *A&A*, 406, 304
- Schreiber, M. R., Nebot Gomez-Moran, A., & Schwöpe, A. D. 2007, in *15th European Workshop on White Dwarfs*, ed. R. Napiwotzki, & M. R. Burleigh, *ASP Conf. Ser.*, 372, 459
- Schreiber, M. R., Gänsicke, B. T., Southworth, J., Schwöpe, A. D., & Koester, D. 2008, *A&A*, 484, 441
- Schwöpe, A. D., Nebot Gomez-Moran, A., Schreiber, M. R., & Gänsicke, B. T. 2009, *A&A*, 500, 867
- Silvestri, N. M., Lemagie, M. P., Hawley, S. L., et al. 2007, *AJ*, 134, 741
- Skumanich, A. 1972, *ApJ*, 171, 565
- Smolčić, V., Ivezić, Ž., Knapp, G. R., et al. 2004, *ApJ*, 615, L141
- Taylor, J. H., Fowler, L. A., & McCulloch, P. M. 1979, *Nature*, 277, 437
- Townsley, D. M., & Bildsten, L. 2003, *ApJ*, 596, L227
- Townsley, D. M., & Gänsicke, B. T. 2009, *ApJ*, 693, 1007
- Verbunt, F., & Zwaan, C. 1981, *A&A*, 100, L7
- Willems, B., & Kolb, U. 2004, *A&A*, 419, 1057
- Yanny, B., Rockosi, C., Newberg, H. J., et al. 2009, *AJ*, 137, 4377